A Longitudinal Characterization of Perfusion in the Aging Brain and Associations with Cognition and Neural Structure

Adam M. Staffaroni[1], **Yann Cobigo**[1], **Fanny M. Elahi**[1], **Kaitlin B. Casaletto**[1], **Samantha Walters**[1], **Amy Wolf**[1], **Cutter A. Lindbergh**[1], **Howard J. Rosen**[*,1], **Joel H. Kramer**[*,1]

[1]Department of Neurology, Memory and Aging Center, University of California at San Francisco (UCSF), San Francisco, CA, USA

Abstract

Cerebral perfusion declines across the lifespan and is altered in the early stages of several age-related neuropathologies. Little is known, however, about the longitudinal evolution of perfusion in healthy older adults, particularly when perfusion is quantified using magnetic resonance imaging with arterial spin labelling (ASL). The objective was to characterize longitudinal perfusion in typically aging adults and elucidate associations with cognition and brain structure. Adults who were functionally intact at baseline (n=161, ages 47–89) underwent ASL imaging to quantify whole-brain gray matter perfusion; a subset (n=136) had repeated imaging (average follow-up: 2.3 years). Neuropsychological testing at each visit was summarized into executive function, memory, and processing speed composites. Global gray matter volume, white matter microstructure (mean diffusivity), and white matter hyperintensities were also quantified. We assessed baseline associations among perfusion, cognition, and brain structure using linear regression, and longitudinal relationships using linear mixed effects models. Greater baseline perfusion, particularly in the left dorsolateral prefrontal cortex and right thalamus, was associated with better executive functions. Greater whole-brain perfusion loss was associated with worsening brain structure and declining processing speed. This study helps validate noninvasive MRI-based perfusion imaging and underscores the importance of cerebral blood flow in cognitive aging.

Keywords

Corresponding Author: Adam M. Staffaroni, PhD, Assistant Professor, University of California, San Francisco (UCSF), Memory and Aging Center, Department of Neurology, 675 Nelson Rising Lane, Suite 190, San Francisco, CA 94143, Phone: 415-502-7201, Adam.Staffaroni@ucsf.edu.
*Joint last authors.

Introduction

Brain function requires constant cerebral blood flow (CBF) to provide oxygen, energy metabolites, and nutrients, and remove carbon dioxide and cellular waste. Regional control of CBF in the mammalian brain is orchestrated by a coordinated unit of neural, glial, and vascular cells, a mechanism known as neurovascular coupling. Animal models suggest that disruption of the neurovascular unit, which could be secondary to pathology of the neural cells, glial cells, or the vasculature, may be an early event in pathological brain aging (Kisler, Nelson, Montagne, & Zlokovic, 2017). Neurovascular uncoupling has been reported in the early stages of several age-related conditions, including Alzheimer's disease (AD), amyotrophic lateral sclerosis (ALS), and stroke (Bhutani & Anand, 2012; Zlokovic, 2011), and chronic hypoperfusion may incite age-associated cognitive decline and neurodegeneration (de la Torre, 2017; de la Torre, 2012). In vivo markers of CBF are therefore important for understanding and detecting physiological changes of the aging brain, and as potential predictive biomarkers of age-related disease risk.

Until recently, CBF has been quantified directly using radioactive ligands, including [15O] water positron emission tomography (PET). Although not a direct measure of CBF, one of the most common imaging technique for quantifying neural functioning in aging has been [18F] fluorodeoxyglucose (FDG)-PET, which measures glucose metabolism via injection of a radioactive ligand. Because of neurovascular coupling, glucose consumption is tightly coupled with CBF (Baron et al., 1982; Furlow, Harrison, & Harrison, 1983), and [18F]FDG-PET and [15O]water PET are highly correlated (Bentourkia et al., 2000; Fox, Raichle, Mintun, & Dence, 1988). Advances in magnetic resonance imaging (MRI) have permitted direct, noninvasive quantification of CBF through the use of a technique known as arterial spin-labeling (ASL) perfusion imaging. In ASL imaging, rather than using a radioactive tracer as a label, protons in the blood are labeled with a radiofrequency pulse; the perfusion of these magnetically-tagged protons to each voxel of the brain is then recorded. Consistent results have been observed between [15O]water PET and ASL (Feng et al., 2004; Ye et al., 2000). Furthermore, joint analyses of [18F]FDG-PET and ASL acquisition have confirmed a good overall correlation between perfusion and glucose uptake in controls (Cha et al., 2013), as well as in patients with Alzheimer's disease (Chen et al., 2011), Lewy body dementia (Nedelska et al., 2018), and frontotemporal dementia (Tosun et al., 2016). Recent work has shown relatively strong correlations between ASL imaging and relative perfusion (R1) quantified during dynamic Pittsburgh Compound B (PiB) PET imaging in carriers of autosomal dominant AD mutations (Yan et al., 2018).

In accordance with animal studies of neurovascular coupling, glucose metabolism and CBF in the human brain appears to change early in pathological aging and may assist in predicting clinical course. For example, decreased metabolism detected using [18F]FDG-PET has long been observed as an early change in AD (Minoshima et al., 1997; Reiman et al., 2004), and several studies have described its utility for predicting conversion to dementia (Choo et al., 2013; Iaccarino et al., 2017; Prestia et al., 2013). Generally, studies using ASL have been consistent with the [18F]FDG-PET literature. For example, Iturria-Medina and colleagues (Iturria-Medina et al., 2016) found that hypoperfusion was one of the earliest manifestations of late-onset AD in a large sample from ADNI, building on prior work

showing ASL-quantified CBF was sensitive to changes in MCI and early AD (for review, see Zhang, Gordon, & Goldberg, 2017). Lower whole-brain CBF measured using ASL has also been shown to predict faster cognitive decline in AD (Benedictus et al., 2017) and conversion from mild cognitive impairment (MCI) to dementia (Chao et al., 2010).

Despite these studies pointing to perfusion as an early biomarker of pathological aging, there has been little research on the natural history and cognitive correlates of ASL perfusion in functionally intact older adults. The majority of studies are cross-sectional and have established that perfusion reductions occur with increasing age (Asllani et al., 2009; Chen, Rosas, & Salat, 2011; Parkes, Rashid, Chard, & Tofts, 2004; Zhang et al., 2017). Only two studies to date have characterized ASL and cognition with repeated measures in this population; both included baseline measurements of ASL only. De Vis and colleagues studied 115 healthy adults over age 54 with a single perfusion image at baseline and follow up cognitive testing (De Vis et al., 2018). They showed that higher whole-brain and frontal CBF predicted better cognition roughly four years later, particularly episodic memory. Similarly, Xekardarki and colleagues found that baseline CBF, particularly in the posterior cingulate cortex (PCC), was lower in those older adults who showed cognitive decline at follow-up (Xekardaki et al., 2015).

Although early evidence indicates that ASL may be a promising, non-invasive method for studying aging, there is much we do not know. For example, there is little knowledge about longitudinal, within-person changes in ASL perfusion, and there are no studies to our knowledge with concurrent, longitudinal ASL and longitudinal assessment of cognition. Moreover, few if any studies have determined whether ASL imaging explains additional variance in cognition above and beyond standard structural imaging modalities. The present study sought to understand perfusion changes and their contributions to cognitive aging. First, we aimed to establish the natural history of gray matter perfusion changes in older adults by characterizing its longitudinal trajectory in a typically aging cohort with longitudinal perfusion imaging. We next examined cross-sectional and longitudinal associations with several domains of cognition commonly affected in aging: memory, executive functions, and processing speed. We assessed for convergent validity by examining the association of ASL perfusion with well-established structural imaging: gray matter volume, diffusion tensor imaging, and white matter hyperintensities (WMH). We also examined the potential for baseline perfusion to predict trajectories of cognition and brain structure. Together, these analyses will help clarify the utility of CBF as an early marker of cognitive aging, explore ASL's utility as a risk-stratification tool based on its ability to predict adverse trajectories, and may shed light on the neurobiology of cognitive aging.

Materials and Methods

Participants

Functionally intact older adults from the Hillblom Aging Network cohort with perfusion imaging were enrolled in the study. The Hillblom Aging Network cohort consists of community-dwelling older adults recruited at the University of California, San Francisco (UCSF), Memory and Aging Center as part of a larger longitudinal study that recruits adults over age 40. The sample included neurologically and functionally intact older adults at

baseline who received at least one time point of perfusion imaging. All participants were reviewed at a case conference with a board-certified neuropsychologist (JHK) and neurologist. The neurologic and neuropsychological examination was used to determine that participants were neurologically normal. Informant interview (Clinical Dementia Rating Scale, CDR) was also used. Baseline exclusion criteria included syndromic diagnosis of dementia or mild cognitive impairment (MCI) according to consensus research criteria (Albert et al., 2011; McKhann et al., 2011), neurological conditions that may affect cognition (e.g. epilepsy, stroke, Parkinson's disease), significant systemic medical illnesses, severe psychiatric illness (e.g. bipolar disorder, schizophrenia), a substance use disorder within 20 years, or current moderate to severe depression (Geriatric Depression Scale   15 of 30). We also excluded those with a high degree of white matter pathology as measured by a Fazekas score of 3 (Fazekas, Chawluk, Alavi, Hurtig, & Zimmerman, 1987). This resulted in a sample of 161 participants with 325 total observations; 136 had repeated neuroimaging. A small subset (n = 11, 6.8%) of the sample began showing some cognitive or neurologic change across the course of the study; 10 were diagnosed with MCI (5 amnestic, 4 mixed, 1 language) and 1 with Parkinson's disease. These participants were left in the study in order to mimic the predictions associated with someone who is functionally-intact at the time of study enrollment/presentation to the clinic, but we controlled for converter status. Demographic data, baseline cognition, and information about follow-ups are provided in Table 1. As shown in Table 2, not all participants had all imaging modalities, particularly WMH. Multivariate comparisons were conducted in samples with overlapping data. All participants provided written informed consent and the UCSF Committee on Human Research approved the study protocol.

Cognitive Measures

Neuropsychological constructs were assessed using paper and pencil and computerized batteries of the primary cognitive domains that decline with aging: processing speed, executive functions, and episodic memory. Processing speed was analyzed using a previously described computerized battery that is sensitive in an aging population and is associated with brain structure (Kerchner et al., 2012) and function (Staffaroni et al., 2018). Episodic memory tasks included the California Verbal Learning Test, 2nd edition (Dean C. Delis, Kramer, Kaplan, & Ober, 2000), short delay free recall, long delay free recall, and recognition discriminability (d'), as well as the total score on Benson figure recall from the Uniform Data Set (Weintraub et al., 2018). Executive function tests included correct lines per minute on a modified version of the trail making test (Kramer et al., 2003), longest digit span backward, total correct on Design Fluency, Condition 1 from the Delis-Kaplan Executive Function System (DKEFS; Delis *et al.*, 2001), and total correct on the Stroop Interference task (Stroop, 1935). Each test was converted to a Z-score and the resultant Z-scores were averaged for each participant to create executive function and episodic memory composites as previously described (Staffaroni et al., 2018).

Neuroimaging

Scanner—Magnetic resonance imaging data were acquired on a 3T Trio scanner (Siemens Medical Systems, Erlangen, Germany). Volumetric MPRAGE sequences at UCSF was used to acquire T1-weighted images of the entire brain (Sagittal slice orientation; slice thickness

= 1.0mm; slices per slab = 160; in-plane resolution = 1.0×1.0mm; matrix = 240×256; TR = 2300ms; TE = 2.98ms; TI = 900ms; flip angle = 9°). Pulsed ASL (PASL) imaging was acquired using QUIPSSII with Thin-slice TI1 Periodic Saturation (Q2TIPS) sequence incorporated in a PICORE (Proximal Inversion with Control of Off-Resonance Effects) labeling scheme (Luh, Wong, Bandettini, & Hyde, 1999). The periodic saturation pulses started at the postlabeling delay inversion time TI1 = 700ms after the in-plan presaturation radio infrequency pulse; the readout started at the postlabeling delay inversion time TI2 = 1800ms. The repetition and echo time were TR/TE = 2500/11ms. We acquired sixteen slices, each 6mm thick with a 7.2mm center to center distance and a matrix 64×56 of 4×4mm^2 in-plane voxel resolution. The Fluid Attenuated Inversion Recovery (FLAIR) MRI imaging was acquired with slice thickness = 1.00mm; slices per slab = 160; in-plane resolution = 0.98×0.98mm; matrix = 256×256; TR = 6000ms; TE = 388ms; TI = 2100ms; flip angle = 120°. The diffusion sequence was acquired using the following parameters: TR/TE 8200/86 ms; B=0 image and 64 directions at B=2000 s/mm^2; FOV 220×220 mm^2 and 2.2 mm thick slices; matrix 100×100 with 60 slices yielding 2.2 mm^3 isotropic voxels / (TR/TE 8000/109 ms; B=0 image and 64 directions at B=2000 s/mm^2; FOV 220×220 mm^2 and 2.2 mm thick slices; matrix 100×100 with 55 slices yielding 2.2 mm^3 isotropic voxels).

Volumetric Imaging—Before processing, all T1-weighted images were visually inspected for quality. Images with excessive motion or image artifact were excluded. Magnetic field bias was corrected using the N3 algorithm (Sled, Zijdenbos, & Evans, 1998). Tissue segmentation was performed using the unified segmentation procedure in SPM12 (Ashburner & Friston, 2005). Each participant's T1-weighted image was warped to create a study-specific template by non-linear registration template generation using Large Deformation Diffeomorphic Metric Mapping (Ashburner & Friston, 2011). Modulated intra-subject gray and white matter were normalized and smoothed (~10mm full width half maximum Gaussian kernel) in the group template. Every step of the transformation was carefully inspected from the native space to the group template. For statistical purposes, linear and non-linear transformations between the group template space and International Consortium of Brain Mapping (ICBM) space were applied (Mazziotta, Toga, Evans, Fox, & Lancaster, 1995). Quantification of volumes in specific brain regions at each time point was accomplished by transforming a standard parcellation atlas (Desikan et al., 2006) into ICBM space and summing all modulated gray matter within each parcellated region. Total intracranial volume (TIV) was estimated for each subject in MNI space (Malone et al., 2015). Gray matter volume (GMV) and TIV are reported in cm^3.

ASL Perfusion—ASL data was processed to obtain partial volume corrected maps of gray matter perfusion as previously described (Du et al., 2006; Hayasaka et al., 2006; Johnson et al., 2005). Frames of the ASL acquisition were corrected for motion, co-registered with the first frame (M0) using FSL (Jenkinson, Beckmann, Behrens, Woolrich, & Smith, 2012), and differential perfusion images were created by subtracting unlabeled from adjacent labeled frames and averaging these subtraction images (Aguirre, Detre, Zarahn, & Alsop, 2002). Susceptibility artifacts along the phase-encoding direction were corrected in the M0 frame and perfusion map using ANTs SyN (Avants, Epstein, Grossman, & Gee, 2008) restricted to the coronal axis. An automatic quality control process removed tagged/untagged pair of

frames when the relative root mean square (RMS) distance value between two consecutive frames was higher than 0.5 mm. The participant was dropped if this RMS value was higher than 1 mm. CBF was calculated by applying the Buxton kinetic model to the perfusion map (Buxton et al., 1998; Wang et al., 2003). Partial volume correction was based on the tissue segmentation maps from MPRAGE using the transformation matrix from T1 to M0 (Du et al., 2006; Müller-Gärtner et al., 1992). All CBF images were visually inspected in the native and study-specific template; analyses were conducted in a study-specific template. Finally, for the purposes of visualization, images were transformed into MNI space to verify anatomical localization and for creation of figures, because most standard atlases and templates are in MNI space. Poor quality images that were out of the field of view, or contained large susceptibility or motion artifacts were removed from the study. The CBF maps were partial volume corrected (PVC) in the gray matter at each timepoint in their native space. After applying the structural registration transformations to the CBF PVC maps, the maps were masked using voxels from the group template with 50% probability of being gray matter; cerebellar voxels were excluded. A global CBF value was calculated that averaged all voxels in this mask.

Diffusion Tensor Imaging (DTI)—Our DTI pipeline has been described previously (Elahi et al., 2017). Briefly, FSL (Jenkinson et al., 2012) software was used to co-register the diffusion direction images with the b = 0 image, then a gradient direction eddy current and distortion correction were applied. Diffusion tensors were calculated using a non-linear least-squares algorithm from Dipy (Garyfallidis et al., 2014). After quality control, participants' tensors were registered linearly and non-linearly into a common space using DTI-TK (Zhang, Yushkevich, Alexander, & Gee, 2006), and whole-brain white matter mean diffusivity (MD) values were extracted.

White Matter Hyperintensities (WMH)—WMHs were quantified using a previously-described, automated algorithm (Staffaroni et al., 2018) based on a regression algorithm (Dadar et al., 2017) using Hidden Markov Random Field with Expectation Maximization software (Avants, Tustison, Wu, Cook, & Gee, 2011). Global WMH burden in mm^3 was log transformed to achieve a normal distribution.

Statistical Analyses

Cross-Sectional Analyses—Baseline associations between whole-brain gray matter ASL CBF and variables of interest were analyzed by fitting linear regression models. To understand the associations with age, education, and gender, all three were entered as simultaneous predictors of CBF. For the primary analyses with cognition and brain structure, CBF was entered as an independent variable. Standardized beta (*ß)* and unstandardized (*b*) estimates are presented for linear regression models. Age, sex, and education were included in all analyses that included neuropsychological variables, and age, sex, and total intracranial volume (TIV) in those models that included structural imaging. Converter status (dummy-coded) was included in the longitudinal models.

In a follow up analysis, we conducted voxel-wise analyses to explore the spatial associations between cognition and CBF. The voxel-wise maps were created with general linear models

(Jenkinson et al., 2012), using the baseline, partial volume corrected CBF in the gray matter as the response. The explanatory variables were cognitive composite score, age, education, and TIV. The correction for multiple comparisons used 10,000 permutations (Winkler, Ridgway, Webster, Smith, & Nichols, 2014). Statistically significant areas were selected using threshold-free cluster enhancement for a p-value < 0.05.

Longitudinal Analyses—We fitted linear mixed effects (LME) models with random slopes and intercepts for the longitudinal analyses. We first analyzed longitudinal perfusion changes by including time from baseline (continuous variable) as a fixed and random effect. We next analyzed whether individual longitudinal trajectories were modified by demographics by fitting an LME model with age, education, sex and their interactions with time. We also assessed whether longitudinal changes in CBF were associated with longitudinal changes in cognition and structural imaging variables. Following Neuhaus et al. (Neuhaus & Kalbfleisch, 1998; Neuhaus & McCulloch, 2006), we decomposed whole-brain CBF into within- (time-varying) and between-subject (time-invariant) components to directly relate purely within-subject change in CBF with changes in cognition and structural imaging and to avoid estimation bias resulting from incorrectly assuming common within- and between-subject effects. We first calculated a time-invariant mean CBF across visits for each person. We then subtracted each participant's mean from his/her CBF at each time point to estimate a mean-centered, within-person metric of change. Both were entered as predictors into LME models (along with time), with neuropsychological or neuroimaging variables as the outcomes.

For both cross-sectional and longitudinal models, for any cognitive domains that were significantly associated with within-person changes in CBF at $p < .05$, we assessed whether other structural imaging modalities were also associated with that domain. Any structural modalities that were associated with the cognitive domain of interest at $p < .05$ were modeled simultaneously with CBF to determine relative explanatory contributions. We also ran models without WMH, since a substantive number of participants did not have data for this imaging modality.

Finally, we assessed whether baseline CBF predicted future decline in cognitive and imaging variables by entering baseline CBF as a time invariant predictor. The interaction of baseline CBF and time was our independent parameter of interest in this analysis.

Results

Cross-sectional Relationships at Baseline

Demographics—Demographics are presented in Table 1. Neither age ($\beta = .03$, $b = .03$, $p = .672$) nor education ($\beta = −.08$, $b = −.24$, $p = .336$) were significantly associated with CBF at baseline. Women showed significantly greater global CBF than men ($\beta = .24$, $b = 3.04$, $p = .003$).

Brain Structure—Global CBF was positively associated with global gray matter volume ($\beta = .15$, $b = .15$, $p = .001$) and negatively with global DTI MD ($\beta = −.22$, $b = −.001$, $p = .$

004), shown in Figure 1. The association with WMH was in the expected direction but was not statistically significant ($\beta = -.08$, $b = -.01$, $p = .358$).

Cognition—Greater CBF at baseline was associated with better executive functions ($\beta = .17$, $b = .02$, $p = .031$) as shown in Figure 2 and Table 2. This relationship was slightly weakened ($\beta = .12$, $b = .01$, $p = .198$) after adding MD and WMH to the model ($n = 114$). When only MD and GMV were added ($n = 149$), CBF remained similar in magnitude but was no longer a statistically significant correlate of executive functioning ($b = .01$, $\beta = .15$, $p = .075$). Baseline associations between CBF and processing speed ($\beta = -.11$, $b = -.03$, $p = .250$) and memory ($\beta = .03$, $b = .004$, $p = .738$) were not statistically significant.

We further evaluated the relationship with cognition by conducting a voxel-wise analysis. As shown in Figure 3, greater perfusion in the left frontal lobe, including the dorsolateral prefrontal cortex (dlPFC), and right thalamus were associated with better executive abilities. No voxels were significantly associated with processing speed or memory after controlling for multiple comparisons.

Baseline Perfusion as a Predictor of Future Changes in Cognition and Brain Structure

Baseline perfusion was not significantly associated with future rate of change in any cognitive variables (ps > 0.49). The only relationship with brain structure that reached statistical significance was baseline perfusion predicting the rate of change in global MD values, such that those with *greater* baseline perfusion (z-scored) saw faster subsequent increases in MD (z-score) ($b = .001$, $p = .010$).

Longitudinal Perfusion Analyses

Demographics—Global gray matter perfusion declined annually by 0.66 ml/100g/min ($p < .001$), suggesting that as an individual ages, their perfusion level declines; however, the main effect of age was again non-significant (b = .02, p = .766). Older age was in the direction of being predictive of faster rates of annual perfusion loss (i.e., age by time interaction), but this did not reach statistical significance ($b = -.05$, $p = .071$). Sex ($b = .27$, p = .394) and education ($b = -.03$, $p = .653$) were not statistically significant modifiers of CBF trajectory.

Brain Structure—We observed concordance between the evolution of global perfusion and global structural changes. Within-person reductions in global perfusion were also associated with increasing WMH burden ($b = -.02$, $p = .007$). Within-person reductions in global perfusion were associated with increasing MD ($b = -8.9 \times 10^{-4}$, $p < .001$). Finally, within-person declines in CBF correlated with faster volume loss ($b = .04$, $p = .011$).

Cognition—Greater within-person declines in perfusion were associated with greater slowing of processing speed ($b = -.03$, $p = .039$), but not executive functions ($b = -7.1 \times 10^{-3}$, $p = .339$), or memory (b = -5.5×10^{-3}, $p = .563$).

As outlined in our model building steps, we followed-up on the relationship between CBF and processing speed by evaluating the association of speed with structural imaging modalities (Table 3). Higher overall levels of MD (between-person) were associated with

slower processing speed ($b = 13.68$, $p = .008$), and greater within-person declines in MD were associated with greater slowing of speed, although this did not reach statistical significance ($b = 9.8$, $p = .06$). Neither within-person ($b = -.09$, $p = .236$) nor between-person gray matter volume ($b = -.03$, $p = .318$) was statistically significantly associated with processing speed. Similarly, neither within-person ($b = .41$, $p = .112$) nor between-person WMH burden ($b = .17$, $p = .243$) was significantly associated with processing speed, although both were in the expected direction. In a follow-up analysis, we entered MD and CBF as predictors of processing speed in the subsample (n = 116) that contained both variables. In this subset of the data, the within-person relationship between CBF and speed was again significant ($b = .034$, $p = .033$). After controlling for MD, this relationship was no longer significant ($b = .026$, $p = .135$), with a 24% reduction in the magnitude of the relationship.

Discussion

Changes in CBF may develop during the nascent stages of pathological brain aging, and chronic hypoperfusion might engender adverse cognitive trajectories. Thus, accurate quantification of CBF could be a powerful method for studying the aging brain. MRI-based ASL imaging presents the opportunity to directly quantify CBF with improved spatial resolution, and without the need for injections or exposure to radioactivity, compared to [^{15}O]water PET. Although initial endeavors in healthy and pathological aging have been encouraging, there is a dearth of research making use of longitudinally-acquired ASL imaging and thorough cognitive characterization. The present study directly addresses this gap and provides initial evidence that CBF decreases can be detected in aging using MRI-based ASL imaging. Ultimately, these findings add to our understanding of the neurobiology of cognitive aging.

In our cross-sectional analysis, we found that greater perfusion of the brain's gray matter was associated with better executive functions. When we performed a voxel-wise analysis to further probe the spatial aspects of this relationship, perfusion in the right thalamus and left lateral frontal lobe, including the dlPFC, were demonstrated to be driving this association. The role of the left dlPFC in executive processes has been well-established (Duncan & Owen, 2000), and a prior cross-sectional study of ASL imaging in 52 older adults found frontal perfusion was associated with executive functions and memory (Alosco et al., 2013). A growing body of volumetric (Hughes et al., 2012; Van Der Werf et al., 2001), task-based fMRI (Fan, McCandliss, Fossella, Flombaum, & Posner, 2005; Minzenberg, Laird, Thelen, Carter, & Glahn, 2009), and lesion studies (Carrera & Bogousslavsky, 2006) have together suggested that the thalamus is a critical structure for executive functions and processing speed. Furthermore, our finding that these two particular regions are involved is in concert with the known reciprocal connections between the PFC and thalamus (Sherman, 2016). Evidence is accumulating, particularly in animal models, that suggests this thalamo-prefrontal circuit is integral for executive functions (Ouhaz, Fleming, & Mitchell, 2018; Parnaudeau, Bolkan, & Kellendonk, 2018). Recent work leveraging functional and structural imaging to investigate the brain's connectome suggested that disruption of the fronto-striatal-thalamic circuit may indeed play a key role in human brain aging (Bonifazi et al., 2018).

Longitudinally, we provide some of the first evidence for ASL imaging's potential to study within-person cognitive aging. First, we showed that within-person changes in perfusion were detectable using MRI methods. Longitudinal declines in ASL perfusion were also detected by our group in a recent study of frontotemporal dementia (Staffaroni et al., 2019). The current work further revealed that within-person declines in gray matter CBF were associated with greater deterioration of brain structure as measured by other well-established markers of brain aging: gray matter volume, white matter microstructure integrity, and WMHs. This is consistent with the neurobiological underpinnings of the perfusion signal, since the neurovascular unit comprises several cell types. These results are support a previous cross-sectional study in older adults that found associations among ASL perfusion and gray matter volume and cortical thickness (Alosco et al., 2013). Associations among perfusion, brain volume, WMHs, and cortical microbleeds have also been reported in cross-sectional studies of participants with a variety of vascular risk factors (Crane et al., 2015; Gregg et al., 2015; van Elderen et al., 2011).

Longitudinal declines in perfusion appear to be clinically relevant, as intraindividual reductions in global perfusion were significantly associated with declines in processing speed. We also replicated prior work suggesting that integrity of white matter microstructure, quantified with DTI, is a significant predictor of processing speed (Kerchner et al., 2012). We found that roughly 24% of the relationship between speed and gray matter CBF was explained by white matter integrity. Furthermore, only MD remained a statistically significant predictor of speed when both modalities were modelled together. Together, this confirms that the structural connections between cortical regions play a sizeable role in maintaining processing speed. What might be explaining the other 76% of the relationship between CBF and processing speed? One explanation may have to do with the neurobiology of the perfusion signal. CBF relies on neuronal, glial and vascular health; thus, its ability to capture coordination of multiple cell types (i.e., neurovascular coupling) may be underlying its sensitivity to changes in this cohort.

There is interest in leveraging baseline CBF to predict cognitive trajectories. Neurovascular uncoupling and perfusion changes are among the earliest detectable alterations in age-related brain pathologies, such as cerebrovascular disease and neurodegenerative disease (Iadecola, 2013; Iturria-Medina et al., 2016; Wang et al., 2013; Zlokovic, 2011). Several cross-sectional lifespan studies have established that CBF is generally reduced with age (Asllani et al., 2009; Chen et al., 2011; Lu et al., 2011; Parkes et al., 2004; Zhang et al., 2017). This reduction may be a consequence of a lifetime of cellular damage (de la Torre, 2017) and is exacerbated by vascular risk factors (Bangen et al., 2014), which further decrease blood flow (de la Torre, 2000). Chronic hypoperfusion has been proposed as an inciting event in the pathogenesis of neurodegenerative disease (de la Torre, 2017). A large population based study of 4,759 participants without dementia from the Rotterdam Study found that baseline perfusion levels, quantified phase-contrast images rather than ASL, were associated with accelerated cognitive decline (Wolters et al., 2017). A study of 115 health older adults with baseline ASL CBF and cognitive assessment at a 4-year follow up visit found that perfusion at baseline predicted cognition at the second time point (De Vis et al., 2018), and another found that those older adults who went on to show cognitive declines (n=73) had lower baseline ASL perfusion than their counterparts who remained stable (n=75), particularly in

the PCC (Xekardaki et al., 2015). In the current sample of older adults who were functionally and clinically intact at baseline, we did not replicate the finding that CBF was a significant predictor of subsequent cognitive decline. This null finding could be due to the fact that our sample is quite healthy with a small number of converters/decliners. Thus, there may be a survival bias, such that some of our highly-educated participants have developed high levels of cognitive reserve and brain resilience, limiting variability and reducing power to detect changes in cognitive outcomes over time. Of note, this could also explain the lack of an association between age and CBF in this cohort. The study by De Vis and colleagues also had a longer mean duration (4 years) of follow up time, which could have improved their power to detect an effect. Although follow-up time in the study by Xekardaki and colleagues was 18-months, they used a different methodological approach in which they dichotomized converters and non-converters based on neuropsychological testing and conducted a group comparison, rather than treating rate of decline continuously.

In contrast to our hypothesis, we found that greater CBF predicted faster rates of declining white matter microstructure (i.e., increased MD). Others studies have revealed early *hyper*perfusion, particularly in the medial temporal lobes, in individuals at genetic risk of AD because they carried the APOE ε4a allele (Bangen et al., 2012; Wierenga et al., 2012). It is conceivable that early pathology could lead to increased blood flow, possibly through early network hypersynchronicity (Hillary & Grafman, 2017; Palop & Mucke, 2016). Alternatively, this could simply represent regression to the mean or could be a spurious finding due to multiple comparisons. This study was not designed to specifically look at predicting conversion; based on prior studies, future work should continue to delve into ASL's potential as an early indicator of future cognitive trajectory in cohorts with a larger number of converters, such as ADNI.

Several limitations should be noted. One limitation is the lack of PET-ligands for Alzheimer's disease, the most common proteinopathy of aging. Combining knowledge of participants' amyloid and tau status will help us disentangle how specific pathologies of aging affect the perfusion signal. Second, data in this study was acquired using a 2D PASL acquisition sequence. Some work has suggested that newer 3D and PCASL sequences may have higher signal to noise properties (Dai, Garcia, de Bazelaire, & Alsop, 2008; Wu, Fernández-Seara, Detre, Wehrli, & Wang, 2007). In this study, the absolute global CBF values for some participants are below the levels that are physiologically expected (i.e., < 20 ml/100 mg/min). Extensive validation of the pipeline suggests that this is the result of the acquisition parameters, such that the 1800ms delay time may not be well targeted to capture peak perfusion across our participants. Although these absolute values should not be interpreted as reflecting the exact physiological levels, the relative perfusion values are accurate and allow us to conduct the statistical analyses in this paper. Another limitation is that for some analyses, we took a whole brain approach. This was to limit the number of comparisons and provide the opportunity for a broad characterization of perfusion changes, but hypothesis- and data-driven methods are warranted in follow-up studies. For example, precuneal perfusion has been shown to precede conversion from MCI to AD (Borroni et al., 2006; Hirao et al., 2005). Furthermore, using a whole-brain approach may affect the associations observed between perfusion imaging and other modalities. For example, Chen and colleagues (Chen et al., 2011) showed a dissociation in the regional effects of age on

CBF and gray-matter atrophy. Despite these limitations, this study advances our understanding of cognitive aging and provides early evidence of the utility of MRI-based perfusion imaging.

Conclusion

ASL perfusion may be a powerful technique to study functional brain changes associated with aging. In addition to confirming prior cross-sectional work, this study makes several additions to the literature. First, we found that perfusion of the left lateral frontal lobe and the thalamus supported executive function performance at baseline. Second, we provide evidence that intraindividual declines in perfusion can be quantified in older adults who are functionally intact at their first study visit. Next, we showed that longitudinal reductions in perfusion are associated with slowed processing speed in aging. Finally, our results indicate that longitudinal perfusion loss is associated with changes in several aspects of brain structure, as indexed by DTI, volumetric MRI, and WMHs. Although potentially sensitive to early age-related changes, perfusion imaging is unlikely to be specific to a single pathological substrate, at least when a whole-brain approach is used. Future studies analyzing patterns of hypo- and hyper-perfusion, as well as analyses that combine ASL perfusion with other disease-specific biomarkers, will be critical for validating this methodology and understanding the neurobiology of cognitive aging.

Acknowledgments:

References

Aguirre GK, Detre JA, Zarahn E, & Alsop DC (2002). Experimental Design and the Relative Sensitivity of BOLD and Perfusion fMRI. NeuroImage, 15(3), 488–500. 10.1006/nimg.2001.0990 [PubMed: 11848692]

Alosco ML, Gunstad J, Jerskey BA, Xu X, Clark US, Hassenstab J, … Sweet LH (2013). The adverse effects of reduced cerebral perfusion on cognition and brain structure in older adults with cardiovascular disease. Brain and Behavior, 3(6), 626–636. 10.1002/brb3.171 [PubMed: 24363966]

Ashburner J, & Friston KJ (2005). Unified segmentation. NeuroImage, 26(3), 839–51. 10.1016/j.neuroimage.2005.02.018 [PubMed: 15955494]

Ashburner J, & Friston KJ (2011). Diffeomorphic registration using geodesic shooting and Gauss-Newton optimisation. NeuroImage, 55(3), 954–67. 10.1016/j.neuroimage.2010.12.049 [PubMed: 21216294]

Asllani I, Habeck C, Borogovac A, Brown TR, Brickman AM, & Stern Y (2009). Separating function from structure in perfusion imaging of the aging brain. Human Brain Mapping, 30(9), 2927–35. 10.1002/hbm.20719 [PubMed: 19172645]

Avants BB, Epstein CL, Grossman M, & Gee JC (2008). Symmetric diffeomorphic image registration with cross-correlation: evaluating automated labeling of elderly and neurodegenerative brain. Medical Image Analysis, 12(1), 26–41. 10.1016/j.media.2007.06.004 [PubMed: 17659998]

Avants BB, Tustison NJ, Wu J, Cook PA, & Gee JC (2011). An open source multivariate framework for n-tissue segmentation with evaluation on public data. Neuroinformatics, 9(4), 381–400. 10.1007/s12021-011-9109-y [PubMed: 21373993]

Bangen KJ, Nation DA, Clark LR, Harmell AL, Wierenga CE, Dev SI, … Bondi MW (2014). Interactive effects of vascular risk burden and advanced age on cerebral blood flow. Frontiers in Aging Neuroscience, 6, 159 10.3389/fnagi.2014.00159 [PubMed: 25071567]

Bangen KJ, Restom K, Liu TT, Wierenga CE, Jak AJ, Salmon DP, & Bondi MW (2012). Assessment of Alzheimer's Disease Risk with Functional Magnetic Resonance Imaging: An Arterial Spin Labeling Study. Journal of Alzheimer's Disease, 31(s3), S59–S74. 10.3233/JAD-2012-120292

Baron JC, Lebrun-Grandie P, Collard P, Crouzel C, Mestelan G, & Bousser MG (1982). Noninvasive measurement of blood flow, oxygen consumption, and glucose utilization in the same brain regions in man by positron emission tomography: concise communication. Journal of Nuclear Medicine: Official Publication, Society of Nuclear Medicine, 23(5), 391–9. Retrieved from http://www.ncbi.nlm.nih.gov/pubmed/6978932

Benedictus MR, Leeuwis AE, Binnewijzend MAA, Kuijer JPA, Scheltens P, Barkhof F, … Prins ND (2017). Lower cerebral blood flow is associated with faster cognitive decline in Alzheimer's disease. European Radiology, 27(3), 1169–1175. 10.1007/s00330-016-4450-z [PubMed: 27334014]

Bentourkia M, Bol A, Ivanoiu A, Labar D, Sibomana M, Coppens A, … De Volder AG (2000). Comparison of regional cerebral blood flow and glucose metabolism in the normal brain: effect of aging. Journal of the Neurological Sciences, 181(1–2), 19–28. Retrieved from http://www.ncbi.nlm.nih.gov/pubmed/11099707 [PubMed: 11099707]

Bhutani H, & Anand A (2012). Biomarkers in amyotrophic lateral sclerosis: is there a neurovascular pathway? Current Neurovascular Research, 9(4), 302–9. Retrieved from http://www.ncbi.nlm.nih.gov/pubmed/22873722 [PubMed: 22873722]

Bonifazi P, Erramuzpe A, Diez I, Gabilondo I, Boisgontier MP, Pauwels L, … Cortes JM (2018). Structure-function multi-scale connectomics reveals a major role of the fronto-striato-thalamic circuit in brain aging. Human Brain Mapping, 39(12), 4663–4677. 10.1002/hbm.24312 [PubMed: 30004604]

Borroni B, Anchisi D, Paghera B, Vicini B, Kerrouche N, Garibotto V, … Perani D (2006). Combined 99mTc-ECD SPECT and neuropsychological studies in MCI for the assessment of conversion to AD. Neurobiology of Aging, 27(1), 24–31. 10.1016/j.neurobiolaging.2004.12.010 [PubMed: 16298237]

Buxton RB, Frank LR, Wong EC, Siewert B, Warach S, & Edelman RR (1998). A general kinetic model for quantitative perfusion imaging with arterial spin labeling. Magnetic Resonance in Medicine, 40(3), 383–96. Retrieved from http://www.ncbi.nlm.nih.gov/pubmed/9727941 [PubMed: 9727941]

Carrera E, & Bogousslavsky J (2006). The thalamus and behavior: Effects of anatomically distinct strokes. Neurology, 66(12), 1817–1823. 10.1212/01.wnl.0000219679.95223.4c [PubMed: 16801643]

Cha Y-HK, Jog MA, Kim Y-C, Chakrapani S, Kraman SM, & Wang DJJ (2013). Regional correlation between resting state FDG PET and pCASL perfusion MRI. Journal of Cerebral Blood Flow and Metabolism: Official Journal of the International Society of Cerebral Blood Flow and Metabolism, 33(12), 1909–14. 10.1038/jcbfm.2013.147

Chao LL, Buckley ST, Kornak J, Schuff N, Madison C, Yaffe K, … Weiner MW (2010). ASL Perfusion MRI Predicts Cognitive Decline and Conversion From MCI to Dementia. Alzheimer Disease & Associated Disorders, 24(1), 19–27. 10.1097/WAD.0b013e3181b4f736 [PubMed: 20220321]

Chen JJ, Rosas HD, & Salat DH (2011). Age-associated reductions in cerebral blood flow are independent from regional atrophy. NeuroImage, 55(2), 468–78. 10.1016/j.neuroimage.2010.12.032 [PubMed: 21167947]

Chen Y, Wolk DA, Reddin JS, Korczykowski M, Martinez PM, Musiek ES, … Detre JA (2011). Voxel-level comparison of arterial spin-labeled perfusion MRI and FDG-PET in Alzheimer disease. Neurology, 77(22), 1977–85. 10.1212/WNL.0b013e31823a0ef7 [PubMed: 22094481]

Choo IH, Ni R, Schöll M, Wall A, Almkvist O, & Nordberg A (2013). Combination of 18F-FDG PET and cerebrospinal fluid biomarkers as a better predictor of the progression to Alzheimer's disease in mild cognitive impairment patients. Journal of Alzheimer's Disease: JAD, 33(4), 929–39. 10.3233/JAD-2012-121489 [PubMed: 23047371]

Crane DE, Black SE, Ganda A, Mikulis DJ, Nestor SM, Donahue MJ, & MacIntosh BJ (2015). Gray matter blood flow and volume are reduced in association with white matter hyperintensity lesion burden: a cross-sectional MRI study. Frontiers in Aging Neuroscience, 7, 131 10.3389/fnagi.2015.00131 [PubMed: 26217223]

Dadar M, Pascoal TA, Manitsirikul S, Misquitta K, Fonov VS, Tartaglia MC, … Collins DL (2017). Validation of a Regression Technique for Segmentation of White Matter Hyperintensities in Alzheimer's Disease. IEEE Transactions on Medical Imaging, 36(8), 1758–1768. 10.1109/TMI.2017.2693978 [PubMed: 28422655]

Dai W, Garcia D, de Bazelaire C, & Alsop DC (2008). Continuous flow-driven inversion for arterial spin labeling using pulsed radio frequency and gradient fields. Magnetic Resonance in Medicine, 60(6), 1488–97. 10.1002/mrm.21790 [PubMed: 19025913]

de la Torre J. c. (2017, 3 21). Are Major Dementias Triggered by Poor Blood Flow to the Brain? Theoretical Considerations. (Mecocci P, Ed.)Journal of Alzheimer's Disease: JAD 10.3233/JAD-161266

de la Torre JC (2012). Cardiovascular risk factors promote brain hypoperfusion leading to cognitive decline and dementia. Cardiovascular Psychiatry and Neurology 10.1155/2012/367516

De La Torre JC (2000). Critically attained threshold of cerebral hypoperfusion: The CATCH hypothesis of Alzheimer's pathogenesis. In Neurobiology of Aging (Vol. 21, pp. 331–342). 10.1016/S0197-4580(00)00111-1 [PubMed: 10867218]

De Vis JB, Peng S-L, Chen X, Li Y, Liu P, Sur S, … Lu H (2018). Arterial-spin-labeling (ASL) perfusion MRI predicts cognitive function in elderly individuals: A 4-year longitudinal study. Journal of Magnetic Resonance Imaging, 48(2), 449–458. 10.1002/jmri.25938 [PubMed: 29292540]

Delis DC, Kaplan E, & Kramer JH (2001). Delis-Kaplan Executive Function System (DKEFS): Examiner's manual San Antonio, TX: The Psychological Corporation.

Delis DC, Kramer JH, Kaplan E, & Ober BA (2000). California Verbal Learning Test - second edition. Adult version. Manual San Antonio, Tex.: Psychological Corporation.

Desikan RS, Ségonne F, Fischl B, Quinn BT, Dickerson BC, Blacker D, … Killiany RJ (2006). An automated labeling system for subdividing the human cerebral cortex on MRI scans into gyral based regions of interest. NeuroImage, 31(3), 968–80. 10.1016/j.neuroimage.2006.01.021 [PubMed: 16530430]

Du AT, Jahng GH, Hayasaka S, Kramer JH, Rosen HJ, Gorno-Tempini ML, … Schuff N (2006). Hypoperfusion in frontotemporal dementia and Alzheimer disease by arterial spin labeling MRI. Neurology, 67(7). 10.1212/01.wnl.0000238163.71349.78

Duncan J, & Owen AM (2000). Common regions of the human frontal lobe recruited by diverse cognitive demands. Trends in Neurosciences, 23(10), 475–83. Retrieved from http://www.ncbi.nlm.nih.gov/pubmed/11006464 [PubMed: 11006464]

Elahi FM, Marx G, Cobigo Y, Staffaroni AM, Kornak J, Tosun D, … Rosen HJ (2017). Longitudinal white matter change in frontotemporal dementia subtypes and sporadic late onset Alzheimer's disease. NeuroImage: Clinical, 16 10.1016/j.nicl.2017.09.007

Fan J, McCandliss BD, Fossella J, Flombaum JI, & Posner MI (2005). The activation of attentional networks. NeuroImage, 26(2), 471–479. 10.1016/J.NEUROIMAGE.2005.02.004 [PubMed: 15907304]

Fazekas F, Chawluk JB, Alavi A, Hurtig HI, & Zimmerman RA (1987). MR signal abnormalities at 1.5 T in Alzheimer's dementia and normal aging. AJR. American Journal of Roentgenology, 149(2), 351–6. 10.2214/ajr.149.2.351 [PubMed: 3496763]

Feng C-M, Narayana S, Lancaster JL, Jerabek PA, Arnow TL, Zhu F, … Gao J-H (2004). CBF changes during brain activation: fMRI vs. PET. NeuroImage, 22(1), 443–6. 10.1016/j.neuroimage.2004.01.017 [PubMed: 15110037]

Fox PT, Raichle ME, Mintun MA, & Dence C (1988). Nonoxidative glucose consumption during focal physiologic neural activity. Science (New York, N.Y.), 241(4864), 462–4. Retrieved from http://www.ncbi.nlm.nih.gov/pubmed/3260686

Furlow TW, Harrison LE, & Harrison LE (1983). Simultaneous Measurement of Local Glucose Utilization and Blood Flow in the Rat Brain: An Autoradiographic Method Using Two Tracers Labeled with Carbon-14. Journal of Cerebral Blood Flow & Metabolism, 3(1), 62–66. 10.1038/jcbfm.1983.7 [PubMed: 6822619]

Garyfallidis E, Brett M, Amirbekian B, Rokem A, van der Walt S, Descoteaux M, … Dipy Contributors. (2014). Dipy, a library for the analysis of diffusion MRI data. Frontiers in Neuroinformatics, 8, 8 10.3389/fninf.2014.00008 [PubMed: 24600385]

Gregg NM, Kim AE, Gurol ME, Lopez OL, Aizenstein HJ, Price JC, … Klunk WE (2015). Incidental Cerebral Microbleeds and Cerebral Blood Flow in Elderly Individuals. JAMA Neurology, 72(9), 1021–8. 10.1001/jamaneurol.2015.1359 [PubMed: 26167811]

Hayasaka S, Du A-T, Duarte A, Kornak J, Jahng G-H, Weiner MW, & Schuff N (2006). A non-parametric approach for co-analysis of multi-modal brain imaging data: application to Alzheimer's disease. NeuroImage, 30(3), 768–79. 10.1016/j.neuroimage.2005.10.052 [PubMed: 16412666]

Hillary FG, & Grafman JH (2017). Injured Brains and Adaptive Networks: The Benefits and Costs of Hyperconnectivity. Trends in Cognitive Sciences, 21(5), 385–401. 10.1016/j.tics.2017.03.003 [PubMed: 28372878]

Hirao K, Ohnishi T, Hirata Y, Yamashita F, Mori T, Moriguchi Y, … Asada T (2005). The prediction of rapid conversion to Alzheimer's disease in mild cognitive impairment using regional cerebral blood flow SPECT. NeuroImage, 28(4), 1014–21. 10.1016/j.neuroimage.2005.06.066 [PubMed: 16129627]

Hughes EJ, Bond J, Svrckova P, Makropoulos A, Ball G, Sharp DJ, … Counsell SJ (2012). Regional changes in thalamic shape and volume with increasing age. NeuroImage, 63(3), 1134–42. 10.1016/j.neuroimage.2012.07.043 [PubMed: 22846656]

Iaccarino L, Chiotis K, Alongi P, Almkvist O, Wall A, Cerami C, … Perani D (2017). A Cross-Validation of FDG- and Amyloid-PET Biomarkers in Mild Cognitive Impairment for the Risk Prediction to Dementia due to Alzheimer's Disease in a Clinical Setting. Journal of Alzheimer's Disease, 59(2), 603–614. 10.3233/JAD-170158

Iadecola C (2013). The Pathobiology of Vascular Dementia. Neuron, 80(4), 844–866. 10.1016/j.neuron.2013.10.008 [PubMed: 24267647]

Iturria-Medina Y, Sotero RC, Toussaint PJ, Mateos-Pérez JM, Evans AC, Alzheimer's Disease Neuroimaging Initiative, M. W., … Furst AJ (2016). Early role of vascular dysregulation on late-onset Alzheimer's disease based on multifactorial data-driven analysis. Nature Communications, 7, 11934 10.1038/ncomms11934

Jenkinson M, Beckmann CF, Behrens TEJ, Woolrich MW, & Smith SM (2012). FSL. NeuroImage, 62(2), 782–90. 10.1016/j.neuroimage.2011.09.015 [PubMed: 21979382]

Johnson NA, Jahng G-H, Weiner MW, Miller BL, Chui HC, Jagust WJ, … Schuff N (2005). Pattern of cerebral hypoperfusion in Alzheimer disease and mild cognitive impairment measured with arterial spin-labeling MR imaging: initial experience. Radiology, 234(3), 851–9. 10.1148/radiol.2343040197 [PubMed: 15734937]

Kerchner GA, Racine CA, Hale S, Wilheim R, Laluz V, Miller BL, & Kramer JH (2012). Cognitive Processing Speed in Older Adults: Relationship with White Matter Integrity. PLoS ONE, 7(11), e50425 10.1371/journal.pone.0050425 [PubMed: 23185621]

Kisler K, Nelson AR, Montagne A, & Zlokovic BV (2017). Cerebral blood flow regulation and neurovascular dysfunction in Alzheimer disease. Nature Reviews Neuroscience, 18(7), 419–434. 10.1038/nrn.2017.48 [PubMed: 28515434]

Kramer JH, Jurik J, Sha SJ, Rankin KP, Rosen HJ, Johnson JK, & Miller BL (2003). Distinctive neuropsychological patterns in frontotemporal dementia, semantic dementia, and Alzheimer disease. Cognitive and Behavioral Neurology: Official Journal of the Society for Behavioral and Cognitive Neurology, 16(4), 211–8. Retrieved from http://www.ncbi.nlm.nih.gov/pubmed/14665820 [PubMed: 14665820]

Lu H, Xu F, Rodrigue KM, Kennedy KM, Cheng Y, Flicker B, … Park DC (2011). Alterations in cerebral metabolic rate and blood supply across the adult lifespan. Cerebral Cortex (New York, N.Y.: 1991), 21(6), 1426–34. 10.1093/cercor/bhq224

Luh WM, Wong EC, Bandettini PA, & Hyde JS (1999). QUIPSS II with thin-slice TI1 periodic saturation: a method for improving accuracy of quantitative perfusion imaging using pulsed arterial spin labeling. Magnetic Resonance in Medicine, 41(6), 1246–54. Retrieved from http://www.ncbi.nlm.nih.gov/pubmed/10371458 [PubMed: 10371458]

Malone IB, Leung KK, Clegg S, Barnes J, Whitwell JL, Ashburner J, … Ridgway GR (2015). Accurate automatic estimation of total intracranial volume: a nuisance variable with less nuisance. NeuroImage, 104, 366–72. 10.1016/j.neuroimage.2014.09.034 [PubMed: 25255942]

Mazziotta JC, Toga AW, Evans A, Fox P, & Lancaster J (1995). A probabilistic atlas of the human brain: theory and rationale for its development. The International Consortium for Brain Mapping (ICBM). NeuroImage, 2(2), 89–101. Retrieved from http://www.ncbi.nlm.nih.gov/pubmed/9343592 [PubMed: 9343592]

Minoshima S, Giordani B, Berent S, Frey KA, Foster NL, & Kuhl DE (1997). Metabolic reduction in the posterior cingulate cortex in very early Alzheimer's disease. Annals of Neurology, 42(1), 85–94. 10.1002/ana.410420114 [doi] [PubMed: 9225689]

Minzenberg MJ, Laird AR, Thelen S, Carter CS, & Glahn DC (2009). Meta-analysis of 41 Functional Neuroimaging Studies of Executive Function in Schizophrenia. Archives of General Psychiatry, 66(8), 811 10.1001/archgenpsychiatry.2009.91 [PubMed: 19652121]

Müller-Gärtner HW, Links JM, Prince JL, Bryan RN, McVeigh E, Leal JP, … Frost JJ (1992). Measurement of radiotracer concentration in brain gray matter using positron emission tomography: MRI-based correction for partial volume effects. Journal of Cerebral Blood Flow and Metabolism: Official Journal of the International Society of Cerebral Blood Flow and Metabolism, 12(4), 571–83. 10.1038/jcbfm.1992.81

Nedelska Z, Senjem ML, Przybelski SA, Lesnick TG, Lowe VJ, Boeve BF, … Kantarci K (2018). Regional cortical perfusion on arterial spin labeling MRI in dementia with Lewy bodies: Associations with clinical severity, glucose metabolism and tau PET. NeuroImage: Clinical, 19, 939–947. 10.1016/j.nicl.2018.06.020 [PubMed: 30003031]

Neuhaus JM, & Kalbfleisch JD (1998). Between- and within-cluster covariate effects in the analysis of clustered data. Biometrics, 54(2), 638–45. Retrieved from http://www.ncbi.nlm.nih.gov/pubmed/9629647 [PubMed: 9629647]

Neuhaus JM, & McCulloch CE (2006). Separating between- and within-Cluster Covariate Effects by Using Conditional and Partitioning Methods. Journal of the Royal Statistical Society. Series B (Statistical Methodology), 68(5), 859–872. Retrieved from http://www.jstor.org/stable/3879278

Ouhaz Z, Fleming H, & Mitchell AS (2018). Cognitive Functions and Neurodevelopmental Disorders Involving the Prefrontal Cortex and Mediodorsal Thalamus. Frontiers in Neuroscience, 12, 33 10.3389/fnins.2018.00033 [PubMed: 29467603]

Palop JJ, & Mucke L (2016). Network abnormalities and interneuron dysfunction in Alzheimer disease. Nature Reviews Neuroscience, 17(12), 777–792. 10.1038/nrn.2016.141 [PubMed: 27829687]

Parkes LM, Rashid W, Chard DT, & Tofts PS (2004). Normal cerebral perfusion measurements using arterial spin labeling: reproducibility, stability, and age and gender effects. Magnetic Resonance in Medicine, 51(4), 736–43. 10.1002/mrm.20023 [PubMed: 15065246]

Parnaudeau S, Bolkan SS, & Kellendonk C (2018). The Mediodorsal Thalamus: An Essential Partner of the Prefrontal Cortex for Cognition. Biological Psychiatry, 83(8), 648–656. 10.1016/j.biopsych.2017.11.008 [PubMed: 29275841]

Prestia A, Caroli A, van der Flier WM, Ossenkoppele R, Van Berckel B, Barkhof F, … Frisoni GB (2013). Prediction of dementia in MCI patients based on core diagnostic markers for Alzheimer disease. Neurology, 80(11), 1048–56. 10.1212/WNL.0b013e3182872830 [PubMed: 23390179]

Reiman EM, Chen K, Alexander GE, Caselli RJ, Bandy D, Osborne D, … Hardy J (2004). Functional brain abnormalities in young adults at genetic risk for late-onset Alzheimer's dementia. Proceedings of the National Academy of Sciences, 101(1), 284–289. 10.1073/pnas.2635903100

Sherman SM (2016). Thalamus plays a central role in ongoing cortical functioning. Nature Neuroscience, 19(4), 533–41. 10.1038/nn.4269 [PubMed: 27021938]

Sled JG, Zijdenbos AP, & Evans AC (1998). A nonparametric method for automatic correction of intensity nonuniformity in MRI data. IEEE Transactions on Medical Imaging, 17(1), 87–97. 10.1109/42.668698 [PubMed: 9617910]

Staffaroni AM, Brown JA, Casaletto KB, Elahi FM, Deng J, Neuhaus J, … Kramer JH (2018). The Longitudinal Trajectory of Default Mode Network Connectivity in Healthy Older Adults Varies as a Function of Age and is Associated with Changes in Episodic Memory and Processing Speed. The Journal of Neuroscience, 38(11), 3067–17. 10.1523/JNEUROSCI.3067-17.2018

Staffaroni AM, Ljubenkov PA, Kornak J, Cobigo Y, Datta S, Marx G, … Rosen HJ (2019). Longitudinal multimodal imaging and clinical endpoints for frontotemporal dementia clinical trials. Brain, 142(2), 443–459. 10.1093/brain/awy319 [PubMed: 30698757]

Stroop JR (1935). Studies of interference in serial verbal reactions. Journal of Experimental Psychology, 18(6), 643–662.

Tosun D, Schuff N, Rabinovici GD, Ayakta N, Miller BL, Jagust W, … Rosen HJ (2016). Diagnostic utility of ASL-MRI and FDG-PET in the behavioral variant of FTD and AD. Annals of Clinical and Translational Neurology, 3(10), 740–751. 10.1002/acn3.330 [PubMed: 27752510]

Van Der Werf YD, Tisserand DJ, Visser PJ, Hofman PA, Vuurman E, Uylings HB, & Jolles J (2001). Thalamic volume predicts performance on tests of cognitive speed and decreases in healthy aging. A magnetic resonance imaging-based volumetric analysis. Brain Research. Cognitive Brain Research, 11(3), 377–85. Retrieved from http://www.ncbi.nlm.nih.gov/pubmed/11339987 [PubMed: 11339987]

van Elderen SGC, Brandts A, van der Grond J, Westenberg JJM, Kroft LJM, van Buchem MA, … de Roos A (2011). Cerebral perfusion and aortic stiffness are independent predictors of white matter brain atrophy in type 1 diabetic patients assessed with magnetic resonance imaging. Diabetes Care, 34(2), 459–63. 10.2337/dc10-1446 [PubMed: 21216862]

Wang J, Aguirre GK, Kimberg DY, Roc AC, Li L, & Detre JA (2003). Arterial spin labeling perfusion fMRI with very low task frequency. Magnetic Resonance in Medicine, 49(5), 796–802. 10.1002/mrm.10437 [PubMed: 12704760]

Wang Z, Das SR, Xie SX, Arnold SE, Detre JA, Wolk DA, & Alzheimer's Disease Neuroimaging Initiative, A. D. N. (2013). Arterial spin labeled MRI in prodromal Alzheimer's disease: A multi-site study. NeuroImage. Clinical, 2, 630–6. 10.1016/j.nicl.2013.04.014 [PubMed: 24179814]

Weintraub S, Besser L, Dodge HH, Teylan M, Ferris S, Goldstein FC, … Morris JC (2018). Version 3 of the Alzheimer Disease Centers' Neuropsychological Test Battery in the Uniform Data Set (UDS). Alzheimer Disease and Associated Disorders, 32(1), 10–17. 10.1097/WAD.0000000000000223 [PubMed: 29240561]

Wierenga CE, Dev SI, Shin DD, Clark LR, Bangen KJ, Jak AJ, … Bondi MW (2012). Effect of Mild Cognitive Impairment and APOE Genotype on Resting Cerebral Blood Flow and its Association with Cognition. Journal of Cerebral Blood Flow & Metabolism, 32(8), 1589–1599. 10.1038/jcbfm.2012.58 [PubMed: 22549621]

Winkler AM, Ridgway GR, Webster MA, Smith SM, & Nichols TE (2014). Permutation inference for the general linear model. NeuroImage, 92, 381–397. 10.1016/j.neuroimage.2014.01.060 [PubMed: 24530839]

Wolters FJ, Zonneveld HI, Hofman A, van der Lugt A, Koudstaal PJ, Vernooij MW, … Heart-Brain Connection Collaborative Research Group. (2017). Cerebral Perfusion and the Risk of Dementia. Circulation, 136(8), 719–728. 10.1161/CIRCULATIONAHA.117.027448 [PubMed: 28588075]

Wu W-C, Fernández-Seara M, Detre JA, Wehrli FW, & Wang J (2007). A theoretical and experimental investigation of the tagging efficiency of pseudocontinuous arterial spin labeling. Magnetic Resonance in Medicine, 58(5), 1020–7. 10.1002/mrm.21403 [PubMed: 17969096]

Xekardaki A, Rodriguez C, Montandon M-L, Toma S, Tombeur E, Herrmann FR, … Haller S (2015). Arterial spin labeling may contribute to the prediction of cognitive deterioration in healthy elderly individuals. Radiology, 274(2), 490–9. 10.1148/radiol.14140680 [PubMed: 25291458]

Yan L, Liu CY, Wong K-P, Huang S-C, Mack WJ, Jann K, … Wang DJJ (2018). Regional association of pCASL-MRI with FDG-PET and PiB-PET in people at risk for autosomal dominant

Alzheimer's disease. NeuroImage: Clinical, 17, 751–760. 10.1016/j.nicl.2017.12.003 [PubMed: 29527482]

Ye FQ, Berman KF, Ellmore T, Esposito G, van Horn JD, Yang Y, … McLaughlin AC (2000). H(2) (15)O PET validation of steady-state arterial spin tagging cerebral blood flow measurements in humans. Magnetic Resonance in Medicine, 44(3), 450–6. Retrieved from http://www.ncbi.nlm.nih.gov/pubmed/10975898 [PubMed: 10975898]

Zhang H, Yushkevich PA, Alexander DC, & Gee JC (2006). Deformable registration of diffusion tensor MR images with explicit orientation optimization. Medical Image Analysis, 10(5), 764–85. 10.1016/j.media.2006.06.004 [PubMed: 16899392]

Zhang N, Gordon ML, & Goldberg TE (2017). Cerebral blood flow measured by arterial spin labeling MRI at resting state in normal aging and Alzheimer's disease. Neuroscience and Biobehavioral Reviews, 72, 168–175. 10.1016/j.neubiorev.2016.11.023 [PubMed: 27908711]

Zlokovic BV (2011). Neurovascular pathways to neurodegeneration in Alzheimer's disease and other disorders. Nature Reviews Neuroscience, 12(12), 723–738. 10.1038/nrn3114 [PubMed: 22048062]
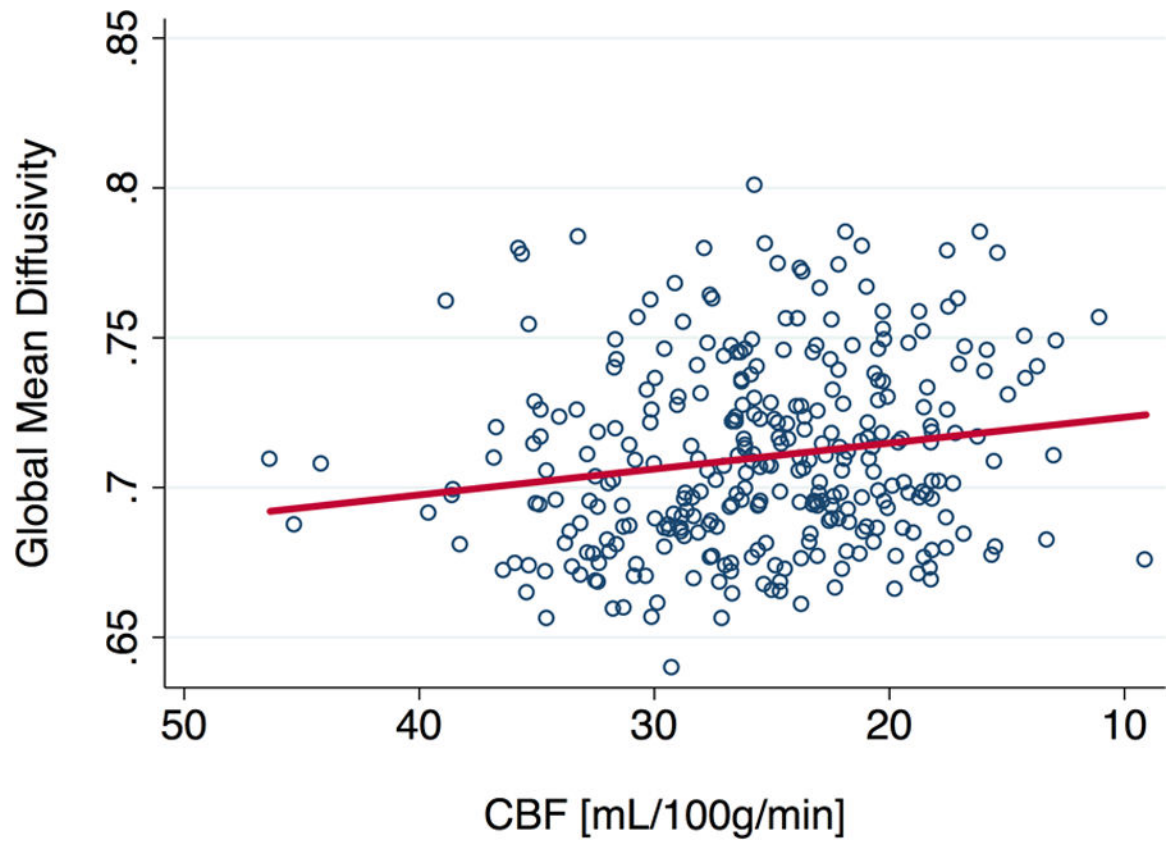
Figure 1.
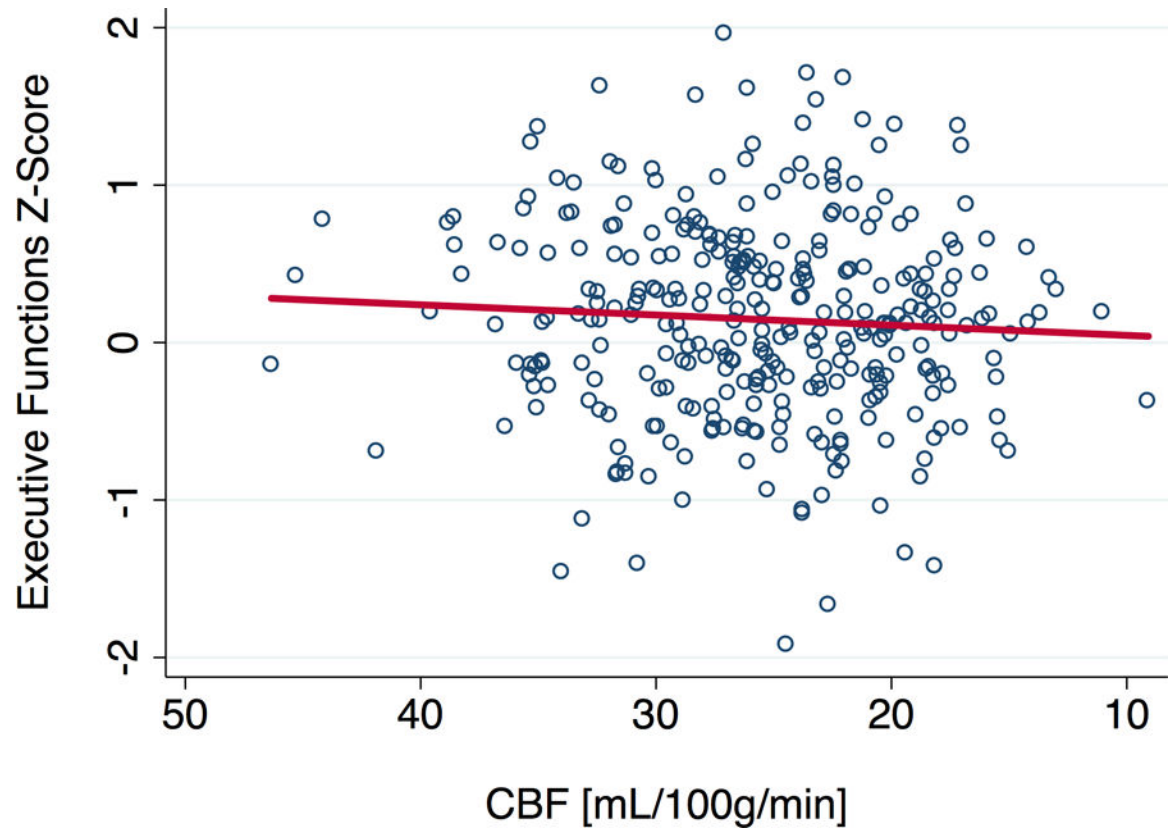CBF at baseline is negatively associated with white matter mean diffusivity.

Figure 2.
CBF at baseline is positively associated with executive functions
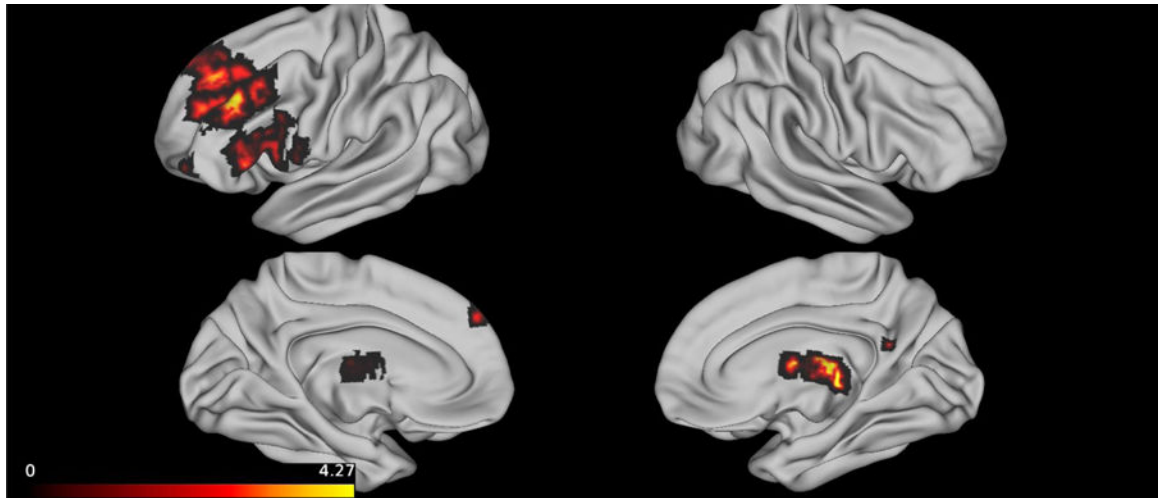
Figure 3.
Greater baseline CBF in the thalamus and left dorsolateral PFC was associated with better executive functions

Note. This figure present cortical projections of voxels that were statistically significantly associated with executive functions after controlling for education, age, and total intracranial volume. Perfusion imaging was restricted to the gray matter and partial volume correction was applied. The heat map presented in the legend corresponds to T statistics. The ROIs from the Harvard-Oxford Cortical Structural parcellation atlas that correspond to the frontal voxels are the left middle, superior, inferior frontal gyri and the frontal pole. The subcortical voxels correspond to the right thalamus.

Table 1.

Baseline study participant demographics, follow-ups, and cognitive characterization

	Mean (SD) or Median (IQR)
Age, years	69.9 (8.3)
Sex, % female	54.7%
Education, years	17.6 (2.1)
Study Visits	2.0 (.6) (range: 1 – 4)
n with multiple visits	141
Cumulative Years Followed	2.3 (1.6) (range: 0 – 5.8)
Years Between Follow-up Visits	2.3 (1.2) (range: .5 – 5.8)
Baseline Cognition	
MMSE	29.2 (29, 30)
Processing Speed, Z-score	2.7 (1.4)
Memory Composite, Z-score	0.1 (0.6)
Executive Composite, Z-Score	0.2 (0.8)

Table 2.

Cross-Sectional, Baseline Correlates of Executive Functions (Z-score)

		Univariate Model				Multivariate Model		
	n	**b coefficient**	**Beta**	**p**	**n**	**b coefficient**	**Beta**	**p**
CBF	155	0.02	0.19	0.016*	114	0.08	0.12	0.198
MD	149	−4.91	−0.2	0.02*	114	−.06	−0.09	0.414
Log WMH	118	−0.17	−0.24	0.013*	114	−.13	−.19	.072
GMV	155	0.01	0.13	0.334	--	--	--	--

*
$p < .05$

Note. In the multivariate models, only listed predictors were included, and all predictors were transformed to sample-based Z-scores, whereas raw predictors were entered into univariate models. As the cross-sectional correlations among CBF, memory, and processing speed were not significant (p .05), we did not analyze multivariate contributions.

Table 3.

Longitudinal Neuroimaging Predictors of Processing Speed Decline (Z-score)

	Univariate Model		Multivariate Model	
	Coefficient	*p*	Coefficient	*p*
CBF: Within Person	−0.03	0.039[*]	−0.16	0.132
CBF: Between-Person	−0.02	0.449	−0.05	0.761
MD: Within Person	9.79	0.06	0.17	0.278
MD: Between-Person	12.73	0.018[*]	0.34	0.030[*]
Log WMH: Within Person	0.4	0.114	--	--
Log WMH: Between-Person	0.14	0.4	--	--
GMV: Within Person	−0.09	0.264	--	--
GMV: Between-Person	−0.03	0.377	--	--

Note. In the multivariate models, only listed predictors were included, and all predictors were transformed to sample-based Z-scores. As the longitudinal associations among CBF, memory, and executive functions were not significant (p .05), we did not analyze multimodal contributions.

[*] $p < .05$